SIMULATION
http://sim.sagepub.com

Finite Element Simulation of a Strong-Post W-Beam Guardrail System

Ali O. Atahan

SIMULATION 2002; 78; 587
DOI: 10.1177/0037549702078010001

The online version of this article can be found at:
http://sim.sagepub.com/cgi/content/abstract/78/10/587

Published by:
SAGE Publications
http://www.sagepublications.com

On behalf of:
SCS
Society for Modeling and Simulation International (SCS)

Finite Element Simulation of a Strong-Post W-Beam Guardrail System

Ali O. Atahan
Department of Civil Engineering
Mustafa Kemal University
Tayfur Sokmen Campus
Serinyol, Hatay, 31040 Turkey
aoatahan@mku.edu.tr

Computer simulation of vehicle collisions has improved significantly over the past decade. With advances in computer technology, nonlinear finite element codes, and material models, full-scale simulation of such complex dynamic interactions is becoming ever more possible. In this study, an explicit three-dimensional nonlinear finite element code, LS-DYNA, is used to demonstrate the capabilities of computer simulations to supplement full-scale crash testing. After a failed crash test on a strong-post guardrail system, LS-DYNA is used to simulate the system, determine the potential problems with the design, and develop an improved system that has the potential to satisfy current crash test requirements. After accurately simulating the response behavior of the full-scale crash test, a second simulation study is performed on the system with improved details. Simulation results indicate that the system performs much better compared to the original design.

Keywords: Computer simulation, LS-DYNA, strong-post guardrail system, cost-effective methods, roadside safety, vehicle collisions

1. Introduction

It is of public interest to develop safer roadways and more crashworthy roadside safety features that minimize the risk of serious injuries and fatalities of vehicle occupants. For the past 60 years, full-scale crash testing has been the most widely accepted means of certifying the impact performance and dynamic characteristics of various roadside safety features. In this method, the design of roadside hardware, such as guardrails, concrete barriers, and crash cushions, is constructed experimentally through an iterative process of design, build, test, redesign, and retest. The cost associated with this method is high, and researchers do not necessarily have complete control over the impact scenarios, test articles, and test conditions. The vehicle fleet has also evolved. Automobiles in use today cover a wider range of sizes and shapes than ever before, and there is a need to use different materials for certain parts of roadside safety hardware. As a result, many of the factors used in the design of roadside safety structures should now be reconsidered. However, it is economically impossible to perform full-scale crash testing on a wide range of parameters.

To evaluate and enhance the crash performance of roadside safety hardware more efficiently, engineers are beginning to rely heavily on sophisticated numerical crash simulations [1]. The primary focus of finite element crash simulations in the roadside safety area has been evaluating the crashworthiness of roadside safety devices. A nonlinear finite element code, LS-DYNA, developed by the Livermore Software Technology Corporation, has become the choice of roadside safety engineers to simulate dynamic three-dimensional motor vehicle impacts of roadside safety structures [2]. When using LS-DYNA, the objective is to make manmade roadside structures and features more crashworthy. It is also intended to ensure that these features are capable of transferring the high-speed collision energy from the colliding vehicle to the feature in a controlled manner so that the vehicle slows or stops, the vehicle remains upright, and the occupants experience minor or no injuries.

In this paper, results of two succeeding simulation studies are presented to demonstrate the capability of LS-DYNA to supplement full-scale crash testing. A strong-post W-beam guardrail system was selected for the study. The system was subjected to full-scale crash testing under the National Cooperative Highway Research Program (NCHRP) Report 350 test 3-11 conditions [3] and failed to meet the requirements. After this crash test, LS-DYNA was used to simulate the impact behavior of the system, pinpoint the potential problem areas, and develop and analyze possible alternatives for improvement. Based on the results

SIMULATION, Vol. 78, Issue 10, October 2002 587-599

of the computer simulations, the crash test performance of the guardrail system improved significantly.

2. Advantages of Computer-Simulated Crash Tests

Recent computer simulation studies of roadside safety devices involve nonlinear finite element programs such as LS-DYNA to model crashes of vehicles with roadside safety features. Since the analysis of roadside safety features involves dynamic loading, inelastic deformations, and nonlinear material behavior with possible failure, the standard linear-elastic analytical methods become incapable of capturing the response behavior accurately.

The high cost of full-scale crash tests greatly limits the number of tests that can be conducted to investigate the safety performance of any roadside safety feature. With computer simulations, however, a variety of impact scenarios that typically cannot be studied by traditional crash-testing methods can be investigated. Using the LS-DYNA, with its material definitions and models, users have the flexibility to simulate a crash from different angles and speeds without the cost of repairing or replacing the structure or vehicle for each test. These impacts can also be graphically viewed from different angles so that users can fully study how the structure or vehicle reacts to complex dynamic forces. Elements, such as the wheel assembly or hood of a car, can be removed to see how internal elements are affected during the impact, which is fairly difficult to study in an actual crash test.

Although it is not feasible to test all of the variations in actual tests, simulations allow more design variations to be analyzed at a fraction of the cost of extensive physical testing. Different impact scenarios, test articles, and test conditions can be easily studied to fully explore the performance of roadside safety features. For example, in Europe, the height of the W-beam in a weak-post guardrail system is slightly lower than that in U.S. practice [4]. The difference in performance can be determined with the use of simulation studies. Furthermore, crash-testing procedures are limited with 25 degrees, while in Europe, most truck accidents occur at an angle greater than 25 degrees [5]. Since no crash tests are performed with such angles, computer simulations become the only option to evaluate the performance of roadside safety features in those cases. Moreover, the effect of real-world conditions such as roadside terrain, which has not been a part of conventional crash-testing procedure, can also be investigated via computer simulations. It is possible to add to these cases when applications of computer simulations greatly improve understanding of the crash performance of roadside safety features.

With the use of simulation results, researchers can assess deficiencies and make adjustments to existing roadside safety features. Simulations also allow optimization of roadside safety hardware and development of improved roadside safety structures. Note that although the increasingly sophisticated finite element codes and advanced computer hardware cannot replace full-scale crash tests altogether, which will always be necessary for validation purposes, computer simulation technology has the potential to reduce the number of crash tests conducted and thus reduce the overall project cost significantly. Also, with the utilization of computer simulation technology, a larger part of the design space can be searched quicker.

3. Description of Roadside Safety Application Studied

3.1 G4(1S) Strong-Post Guardrail System

The G4(1S) strong-post W-beam guardrail system is used extensively in the United States and Europe. In past years, several studies have been undertaken to evaluate the performance of this system. The G4(1S) system evaluated in this study is composed of a W-beam rail supported on W150 × 13 steel posts spaced at 1905 mm. A picture of the system is shown in Figure 1 [6]. The typical post length is 1829 mm, with 1118 mm of the post below grade. Posts are connected with a standard 12-gauge W-beam, which has a nominal thickness of 2 mm. The system uses 356-mm long, W150 × 18 offset blocks between the post and the W-beam to prevent potential wheel snagging on the posts. A 32-mm diameter through bolt is used to connect the flange of the W150 × 18 offset block to the center of W-beam rail.

4. Previous Crash Test

The Texas Transportation Institute has performed a number of full-scale crash tests on the G4(1S) system to evaluate its crashworthiness according to the NCHRP Report 350 test 3-11 procedures. In one of the earlier tests (TTI Test No. 405421-2), a 2000-kg pickup truck traveling at 99.7 km/h and contacting installation at 25.7 degrees failed to meet the NCHRP Report 350 criteria [6]. The vehicle impacted

Figure 1. A picture of the G4(1S) system before crash test 405421-2.

the installation 672 mm upstream of post 17. Even though the system initially contained and partially redirected the vehicle, at approximately 0.345 s into the test, the W-beam rail element ruptured near the splice at post 19, causing the vehicle to penetrate the barrier in an uncontrolled manner.

5. Computer Simulation Study

After the failed crash test, a comprehensive computer simulation study was carried out. The aim was to obtain information about the details of the crash. The study consisted of two steps: the first step involved developing an accurate finite element model for the G4(1S) system, validating the model with the full-scale crash test 405421-2, and thus establishing an accurate baseline model for further evaluation and analysis. In the second step, potential problems resulting from W-beam rail splice rupture and system failure were evaluated, and necessary design changes to the baseline model were implemented.

To perform the simulation studies, a series of finite element models of the G4(1S) strong-post guardrail system was developed. Several models that were previously used and validated were obtained from other sources. The models used in this study include the (1) W-beam rail model, (2) post model, (3) soil model, (4) W-beam boundary conditions, (5) post to W-beam connection model, (6) W-beam splice model, and (7) pickup truck model. Brief explanations of the submodels of the baseline model are given below.

W-Beam Model. Since W-beam material sustains large deformations and possible crushing, large plastic deformations are likely to occur in the W-beam. To account for these effects, a piecewise linear plastic material definition (type 24) was used in LS-DYNA [7]. Table 1 displays the eight stress-strain data points and other parameters used to define the properties of the W-beam material. In addition, a failure criterion based on an ultimate strain was incorporated into the material definition. These parameters were determined based on a series of uniaxial tests. Due to its relatively low thickness, W-beam elements were modeled as 2-D elements defined by unique sets of four nodes. The thickness of W-beam elements is defined separately. The Belyshko-Tsay shell element formulation was used due to its computational efficiency. The number of integration points through thickness was set to 3 to obtain a more accurate simulation. A sketch of a typical four-noded 2-D shell element used in this study along with integration points is shown in Figure 2.

In a crash test, the vehicle typically does not impact the full length of the guardrail. Instead, a small segment, known as the impact region, experiences most of the crushing and transverse displacement. Since it is not cost-effective to model the whole length of the W-beam, in this study, only the W-beam at the impact region was modeled explicitly. Since the length of the impact region has a significant effect on the response behavior of the guardrail model, a sufficiently long guardrail section was modeled. The extent of this region was determined based on both a visual inspection of guardrail installation after the crash test and a detailed simulation study. Based on the analysis, the W-beam was divided into two distinct sections: (1) the region that primarily responded to the impact forces and stresses that resulted from the crash and (2) the region that did not. The region that did not actively partake in resisting impact forces was represented as boundary conditions. The meshing of the W-beam was determined based on a sensitivity study, and an optimum mesh density was used in the model. Details of the mesh sensitivity study for the W-beam are explained in the next section.

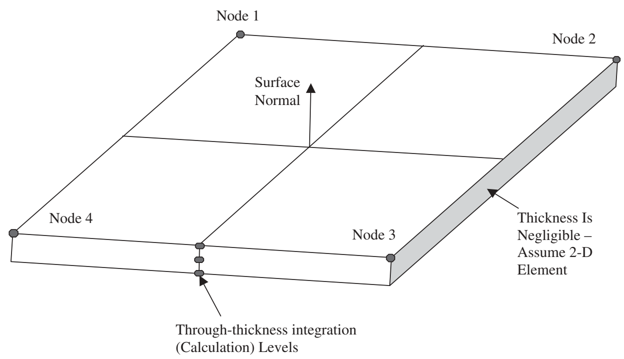

Figure 2. A sketch of a two-dimensional four-noded shell element used in this study with three through-thickness integration levels.

Post and Offset Block Models. Steel posts and offset blocks were also modeled using the piecewise linear plastic material definition, and the properties defining the posts are given in Table 1 [7]. As discussed above, only the posts at the impact region were modeled. Both flanges and webs of W150 × 13 steel posts and W150 × 18 offset blocks were modeled using four-node Belyshko-Tsay shell elements. Figure 3 reveals necessary information about the post and offset block models.

Soil Model. Since it is too computationally demanding to represent soil as a solid element, a well-accepted approximate method was used [8]. Soil was modeled as an array of unidirectional nonlinear springs acting on both cross sections of each post at 100-mm depth intervals. The stiffness of the nonlinear springs increased with depth, and the spring stiffness was defined by the load curves at a specific depth. Figure 4 shows the load deflection curves for some of the springs used in this study. Detailed information about the theory of the soil strength with increased depth and development of curves can be found in a paper by Habibagahi and Langer [9]. The application and line of action of the unidirectional springs on a post are illustrated in Figure 3.

Table 1. LS-DYNA material inputs for W-beam and post/offset block materials

Properties	W-Beam Material		Post/Offset Block Material	
Material type	Piecewise-linear-plastic with failure		Piecewise-linear-plastic with failure	
Element type	Shell		Shell	
Density	7850 kg/m^3		7850 kg/m^3	
Modulus of elasticity	200,000 MPa		200,000 MPa	
Poisson's ratio	0.3		0.3	
Yield stress	450.0 MPa		338.0 MPa	
Failure plastic strain	0.22		∞ (no failure)	
	Effective Plastic Strain	True Stress (MPa)	Effective Plastic Strain	True Stress (MPa)
	0.000	450.0	0.002	338.0
	0.025	508.0	0.026	339.1
	0.049	560.0	0.045	401.2
	0.072	591.0	0.108	490.9
	0.095	613.0	0.203	550.0
	0.140	643.0	0.254	608.2
	0.182	668.0	0.277	657.1
	0.750	840.0	0.300	677.8

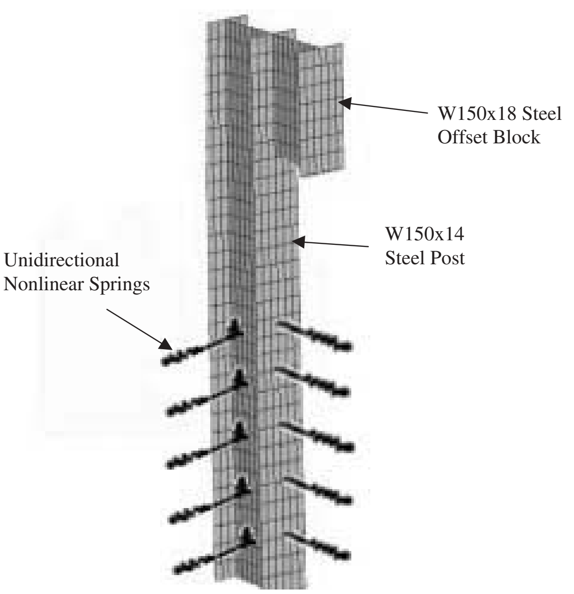

Figure 3. Picture of W150 × 14 post model with unidirectional springs representing soil.

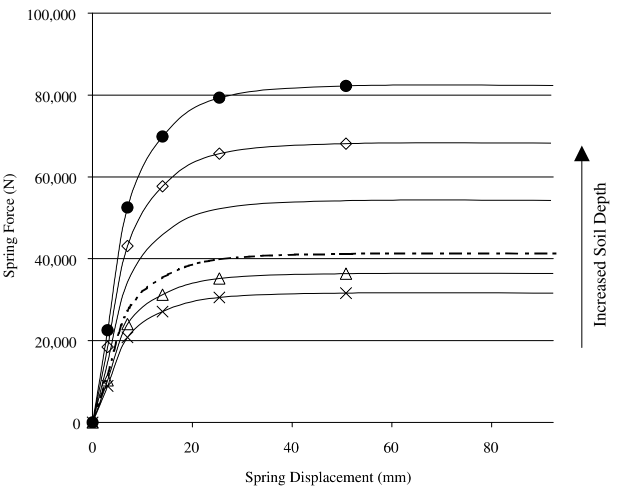

Figure 4. Load deflection curves of unidirectional springs modeling soil.

Boundary Conditions. A portion of the W-beam outside of the impact region serving to anchor the system at both ends was not modeled explicitly to reduce the computational time. After determining the required length of the impact region, as described above, the remainder of the system (including guardrail, posts, and end treatments) located outside was represented as boundary conditions applied to the free ends of the modeled section of the W-beam. Since the W-beam redirects impacting vehicles primarily through beam tension, linear elastic springs were attached to the upstream and downstream ends of the W-beam model to represent boundary conditions [10]. These springs provide rail-end conditions approximating a continuance of the guardrail system both upstream and downstream of the model. The stiffness of the end springs corresponds to the stiffness of the unmodeled section of the W-beam and is calculated from the following relationship:

$$K = \frac{AE}{L}, \quad (1)$$

where K, A, and E are the elastic stiffness of the unmodeled guardrail, the cross-sectional area of the W-beam, and Young's modulus of steel, respectively, and L is the unmodeled length of installation.

Post-to-Rail Connection Model. As described above, a 32-mm diameter bolt is used to connect the post to the center of the W-beam. At the full-scale crash test site, it was observed that all the posts in the impact region of the installation were twisted toward the point of impact. This response was likely caused by the combination of two loading scenarios: the direct torque applied by the post-to-rail bolts arising from the tensile loads in the guardrail and the lateral-torsional buckling induced from the lateral loads applied by the vehicle into the system. Also, several post bolts were significantly deformed in shear and bending modes, and a few became detached from the rail by tearing through the rail slot. A method of approximating the post-to-rail connection in the post model was highly desired because including it explicitly (i.e., details of the bolt shaft, washers, slots, etc.) would significantly increase the required computational time of all subsequent simulations. However, the approximation should closely represent the behavior of the actual bolted connection for various loading modes. Consequently, as shown in Figure 5, an explicit model of the post-to-rail connection was developed. The details of the explicit post-to-rail connection model are shown in Table 2. After testing the model under various loading combinations, including axial, shear, and bending forces, the resulting simulation data were used to validate a simplified connection model. The final simplified connection model was merely a link between post and rail with the properties of the bolted connection.

W-Beam Splice Model. It is a fact that splice connections generate weaker cross sections due to the reduced effective W-beam area at the bolt holes, and these connections are considered prime locations for stress concentrations and possible W-rail ruptures due to bolt-bearing forces. It is also reported that in the full-scale crash test 405421-2, failure initiated at a splice connection resulted in vehicle penetration. However, unlike what is commonly believed, research by Ray et al. [11] has shown that the effect of bolt bearing on holes made a minimal contribution to W-beam rail ruptures. Instead, as discussed later, development of initial imperfections or tears on the W-beam at the offset block–W-beam interface was determined to be the main cause for splice ruptures. Thus, to accurately simulate the W-beam rupture, attention was paid to develop a realistic splice model for the W-beam. After trying out several options, including an explicit bolted connection, as shown in Figure 6, a simple model with an equivalent bolt-opening area on the W-beam was determined to represent

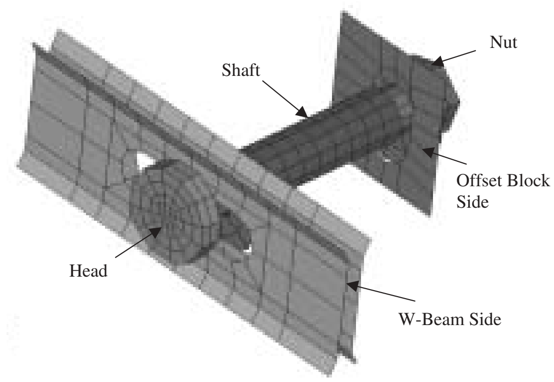

Figure 5. Picture of an explicit post-to-rail connection model.

similar behavior observed in the crash test. A picture of the splice model used in the study is given in Figure 6. It was determined that as long as the splice region interacts with the offset block, the risk of W-beam rupture will always be present. As shown in Table 3, the simple splice model proved to be fairly accurate and immensely cost-effective in simulating failure mechanism at splice connections. Details about the model can be found in a paper by Atahan [12].

Pickup Truck Model. Since its development is beyond the objectives of this paper, the explicit finite element model of the 2000-kg pickup truck was obtained from the National Crash Analysis Center [13]. This detailed version contained approximately 62,340 nodes and 55,800 elements. Due to research needs, several modifications were made to this model. These include remeshing parts that are directly in contact with the W-rail, rotating the tires, changing the element formulation of a few parts, and increasing the shell element warping stiffness to prevent unrealistic penetration problems. All these modifications were necessary to increase the accuracy of the finite element model in capturing the actual crash test performance of the G4(1S) system. As an example, Figure 7 shows an unrealistic penetration problem due to a coarse mesh pattern of the door. The penetration problem was solved after the mesh on the door was refined. Rotating the tires was also necessary to represent real-world conditions. As a result of the rotating tire model, the interaction between the wheel and barrier system improved and provided a more accurate redirection of the vehicle. The effect of changing the shell element warping stiffness in preventing unrealistic penetration problems was also important. These were some of the implications of modifications made on the truck model. More details on the modifications can be found in a report by Atahan [5].

5.1 Mesh Sensitivity Studies

In finite element analysis, the behavior of a model and the interaction between two impacting bodies are significantly

Table 2. Details of explicit post-to-rail connection model

Bolt Component	Number of Elements	Element Type	Material Type in LS-DYNA	Yield Stress (MPa)
Shaft	126	Solid	Type 24	336
Nut	99	Solid	Rigid	NA
Head	90	Solid	Rigid	NA
Washer 1	22	Shell	Type 24	240
Washer 2	22	Shell	Type 24	240

Table 3. Comparison of splice connection models

Splice Type	Number of Elements	Total CPU Time (h:min)	Failure Initiation Time (sec)	Failure Initiation Location	Failure Initiation Strain[a]
TTI Full-Scale Crash Test 405421-2					
—	—	—	0.192	W-beam, below bottom bolt hole	0.22
Finite Element Models					
Explicit splice model	720	6:25	0.184	W-beam, below bottom bolt hole	0.22
Equivalent bolt opening	330	2:34	0.177	W-beam, below bottom bolt hole	0.22

a. Failure initiation strain value was determined from tensile tests performed on coupons taken from the W-beam after the full-scale crash test [12].

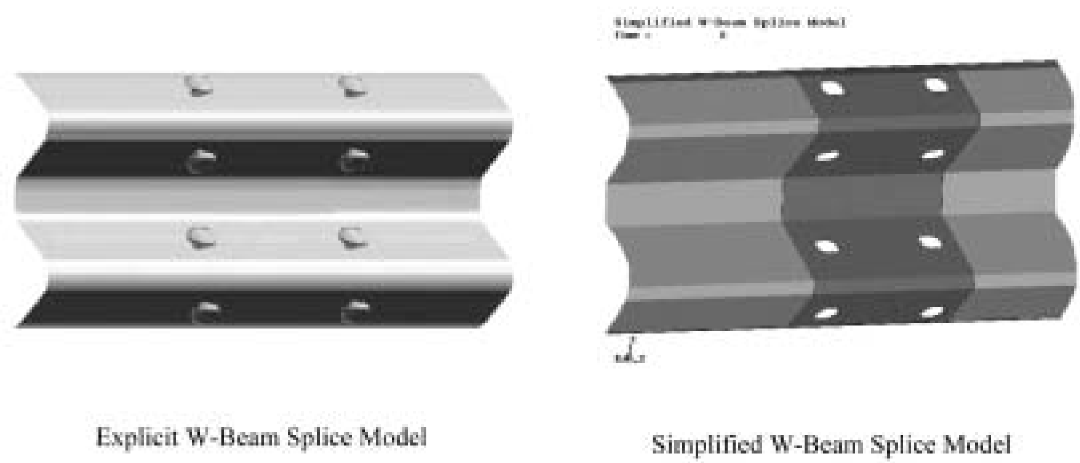

Figure 6. Simplified W-beam splice model used in this study.

dependent on the fineness of the meshings used. Typically, the geometry of the model and the accuracy of the simulation results improve as more elements are used.

However, computational time required for LS-DYNA3D to perform structural analysis also increases with meshing fineness. Consequently, at several steps during this research, diligent effort was made to reduce the number of elements in the G4(1S) finite element model. For this reason, sensitivity studies were conducted on the W-beam rail and post components to optimize the meshings.

A convergence study was performed on the W-beam rail to both determine the sensitivity to meshing density and re-

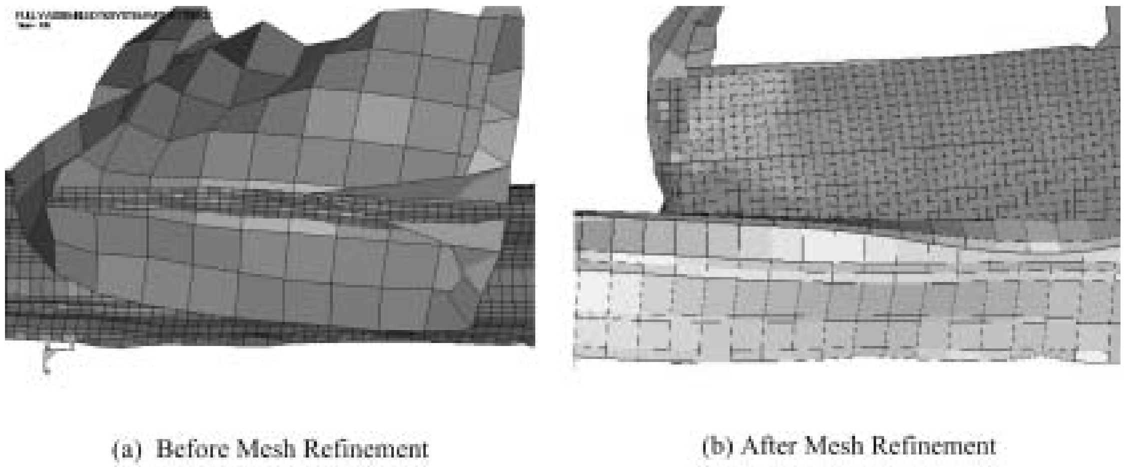

Figure 7. Effect of mesh refinement on penetration of the door model.

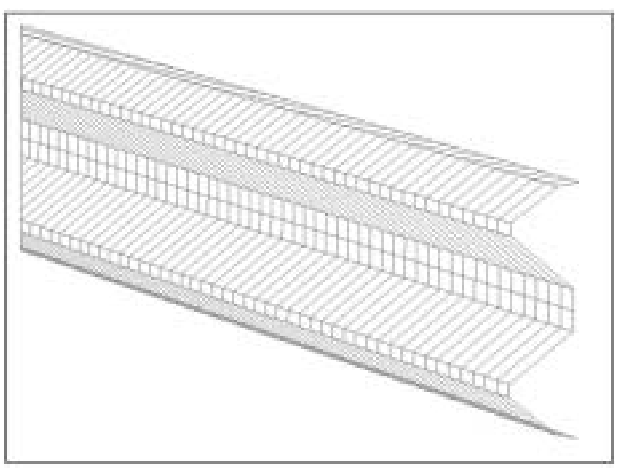

Figure 8. A sample W-beam meshing used in the mesh sensitivity study.

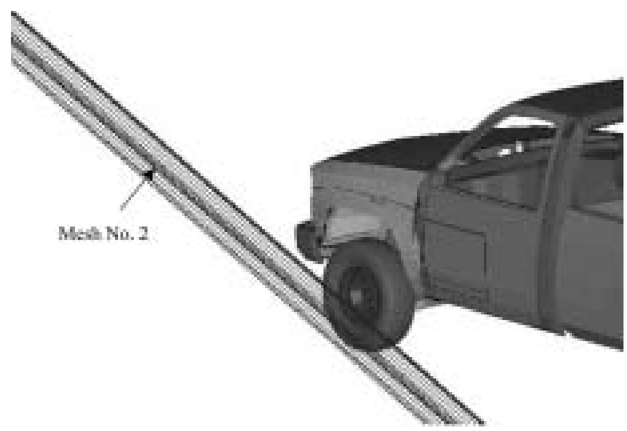

Figure 9. Setup used for the mesh sensitivity study.

duce the number of elements required. The primary meshing parameters investigated were the number of elements around the rail and the maximum aspect ratio. Figure 8 provides an example of a meshing used on this component.

A set of preliminary simulations produced four rail meshings that were analyzed in the sensitivity study. Table 4 summarizes the details of each meshing. To optimize the model of the W-beam rail, the performance using each of these meshings was then evaluated using a pickup truck model with the same overall dimensions and mass as the pickup truck from the latest full-scale crash test. The truck was given a sufficient “height” and vertically centered on the rail cross section. The initial velocity and impact angle also matched test 405421-2. Figure 9 depicts the initial configuration used for simulation in the sensitivity study. Table 4 summarizes results of the four simulations along with full-scale crash test results. As shown in this table, mesh 4 produced the most accurate results in terms of displacements and accelerations. However, due to the large CPU computational time requirements, this meshing was used only at the impact region where large deformations and complex dynamic interactions take place, and mesh 2 was used in the rest of the W-beam model for its cost-effectiveness.

6. Simulation of the Assembled G4(1S) Model

During the development of the G4(1S) model, approximate modeling techniques for many of the G4(1S) system

Table 4. Details of meshings investigated during the rail mesh convergence study

Mesh Number	Total Number of Elements	Maximum Element Aspect Ratio	Total CPU Time (h:min)	Maximum Transverse Displacement of W-Beam (mm)	Maximum Transverse Acceleration 10-ms Average (g's)	Maximum Longitudinal Acceleration 10-ms Average (g's)	Maximum Rail Internal Energy (kJ)
TTI Full-Scale Crash Test 405421-2							
—	—	—	—	1005	−16.7 @ 195 ms 11.1 @ 208 ms	20.81 @ 185 ms	—
Finite Element Models							
1	2646	4.66	6:30	1017	−17.0 @ 180 ms 12.1 @ 200 ms	20.96 @ 197 ms	203.5
2	2860	4.27	4:14	1022	−17.2 @ 181 ms 12.6 @ 204 ms	20.76 @ 100 ms	200.8
3	5720	2.15	6:23	1018	−17.4 @ 188 ms 11.5 @ 197 ms	20.78 @ 83 ms	203.9
4	8360	4.17	14:39	1009	−16.6 @ 193 ms 10.9 @ 206 ms	20.82 @ 106 ms	211.5

Measurements up to W-beam rail rupture time.

components, including various connections and the sections located outside the impact region, were being investigated and developed simultaneously. Once obtained and validated individually, these explicit and simplified models were assembled, thus creating the finite element model for the complete G4(1S) guardrail system. A general view of the final system model is shown in Figure 10. The model was run on a supercomputer under the same full-scale crash test conditions.

7. Evaluation of Baseline Simulation Results

To validate the accuracy of the G4(1S) guardrail model in replicating the full-scale crash test performance, qualitative and quantitative comparisons, including parameters such as velocity and acceleration time histories, event timing, guardrail damage, and guardrail deflections, were made. These comparisons ensured the fidelity of the finite element models for use in further studies with confidence.

Sequential overhead pictures comparing the position of the vehicle and the amount of damage to the guardrail system both for the full-scale crash test 405421-2 and the baseline simulation are depicted in Figure 11. The overall deflected rail shapes, rail rupture times, and the position of the vehicle at the time of rail rupture both in the actual test and the simulation compare well. Comparison of local longitudinal velocity time histories is shown in Figure 12, and they agree well. In addition to these, Table 5 compares the time of W-beam rail rupture, dynamic rail deflection at the time of rail rupture, and guardrail post deflections for the simulation and the actual crash test. As can be seen from this table, results are found to be in good agreement. Figure 13 clearly depicts the potential W-beam rupture initiation point observed in the simulation. When the W-beam failure plastic strain level (represented in Table 1) was reached, elements around this location started to fail, resulting in complete rupture of the W-beam splice. As mentioned later, the reason for the W-beam rupture was the interaction between the sharp edges of offset blocks and the weakened W-beam rail at the splice region. Based on these comparisons, it was concluded that the simulation accurately replicated the response behavior, thus validating the fidelity of finite element models and the baseline simulation study.

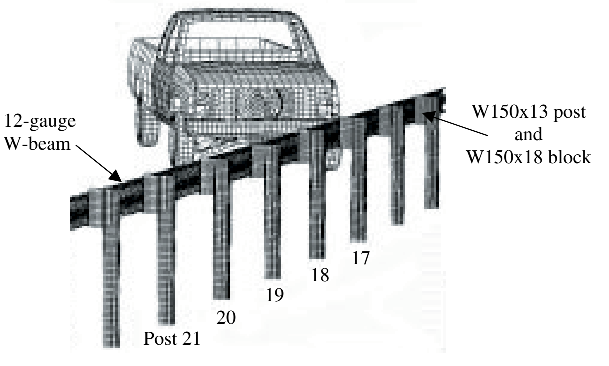

Figure 10. Finite element model of the G4(1S) system used in the baseline simulation study.

8. Improvements to the Baseline Model

After successfully completing the first step and gaining confidence in the fidelity of the baseline G4(1S) model, deficiencies that caused W-beam rupture were investigated. Upon investigation, the reason for rupture at the W-beam splice connection was determined to be the interaction between the steel offset block and the weaker splice region.

Table 5. Comparison for TTI Test 405421-2 versus baseline simulation

Impact Events

	TTI Test 405421-2		Baseline Simulation	
Sequence of Major Events	Time (s)	Speed (km/h)	Time (s)	Speed (km/h)
Initial contact	0.000	99.7	0.000	99.7
Wheel at post 17	0.025	96.2	0.022	96.7
Wheel at post 18	0.087	88.6	0.088	86.3
Time of rail rupture	0.398	47.3	0.389	48.1
Wheel at post 19	0.192	71.1	0.198	73.2
Vehicle parallel with installation	0.214	64.4	0.208	65.2
Uncontrolled vehicle penetration	0.428	41.5	0.431	42.6

Groundline Guardrail Post Deflections

	TTI Test 405421-2		Baseline Simulation	
Post Number	Dynamic (mm)	Permanant (mm)	Dynamic (mm)	Permanant (mm)
16	56	45	54	41
17	121	95	129	102
18	421	pulled out	433	pulled out
19	344	330	357	339
20	230	215	241	221

W-Beam Deflections

	TTI Test 405421-2	Baseline Simulation
Maximum Dynamic Lateral W-Beam Deflection at Time of Rail Rupture (mm)	1005	988

This behavior was clearly observed from the high-speed camera recordings of the crash. During the lateral deflection of the W-beam, the splice region was pushed toward the sharp edges of the steel post. This created an imperfection and a susceptible area for further crack development. Since in test 405421-2, splices are located at posts, the crack easily advanced upwards and eventually ruptured the W-beam rail. The same behavior, which resulted in a similar W-beam splice failure, was also observed and reported in another study [11]. During that test, similar to this case, the splice region was partially wrapped around posts, which resulted in splice damage and a potential rupture initiation point (see Fig. 14). When contacted by the vehicle, the susceptible region containing a crack was severely damaged due to further bending and increased local stresses and finally ruptured. Note that Figure 14 shows results of a full-scale crash test performed on another guardrail system with W-beam splices located at post mid-span [14]. However, this figure is important since it represents the consequences of the presence of sharp edges on unprotected W-beam rail sections.

To improve the performance and prevent potential W-beam splice rupture, in the second simulation, the splice region in the W-beam model was shifted from post to mid-span. The aim was to move an inherently weak W-beam section away from the sensitive post region [11]. The W-beam also was strengthened at post locations to minimize the damaging effects of sharp edges of offset blocks. A 25-cm long sacrificial metal piece with dimensions similar to those of the W-beam was added between the post and the W-beam to protect the W-beam against the development of imperfections and cracks. The properties used for the sacrificial piece are the same as the original W-beam material.

9. Second Simulation Study with Improved Details

After these changes were made, the second simulation study was performed under the same impact conditions. The vehicle contacted the W-beam around 0.000 s, and post 17 and the system began to deform laterally. At around 0.085 s, the front impact side wheel came in contact with post 18, and the post was buckled soon after contact without any considerable deceleration of the vehicle. At this time, the velocity of vehicle was 83 km/h. As the vehicle continued forward, the wheel came in contact with post 19 at around 0.220 s into the simulation. Post 19 was also buckled, and the vehicle continued its forward move with a velocity of 76 km/h. At approximately 0.327 s into the simulation, the vehicle became parallel with the system, showing no potential for penetration into the system. Finally,

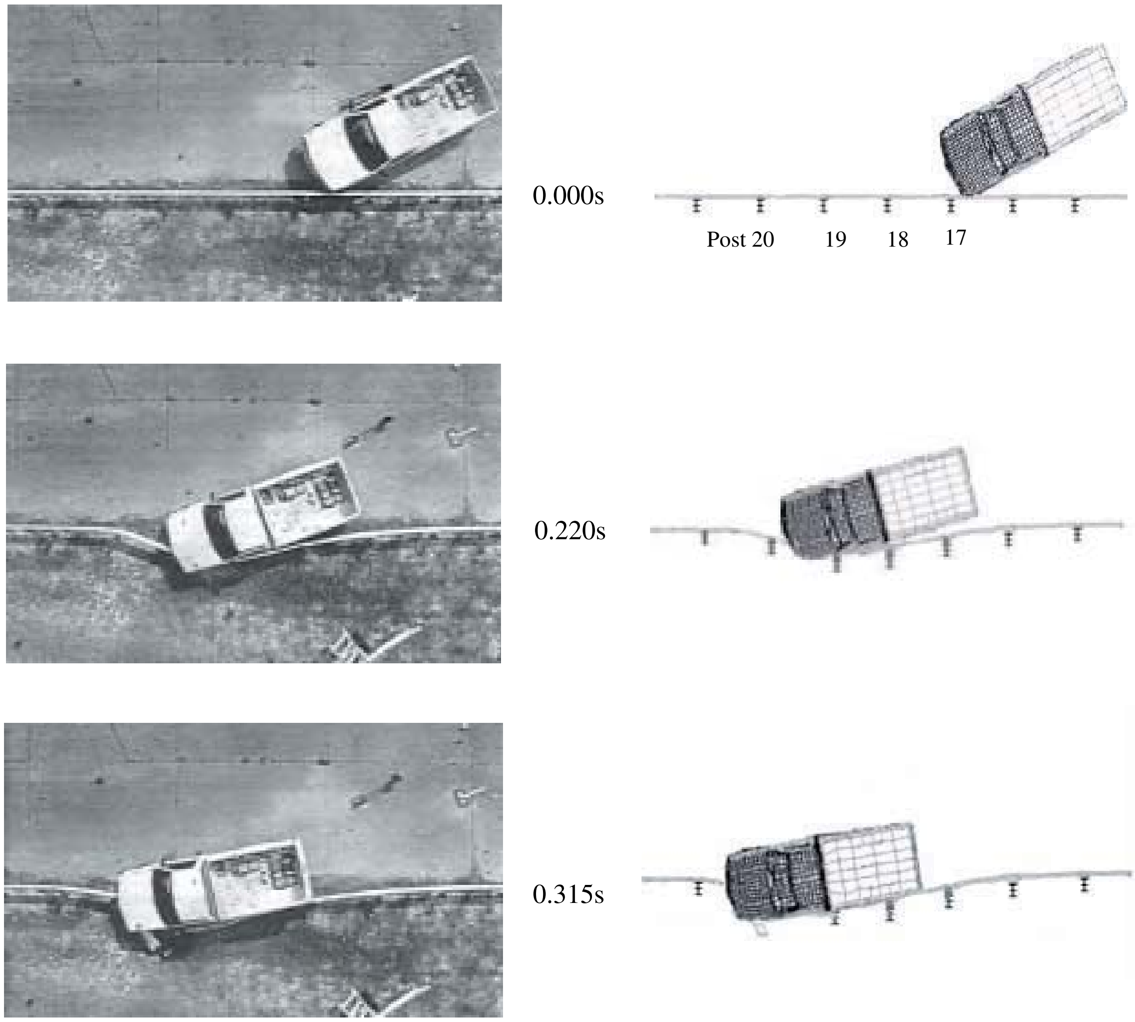

Figure 11. Full-scale crash test 405421-2: Baseline simulation comparison for the G4(1S) system.

the vehicle exited the terminal at approximately 0.520 s with a velocity of 62 km/h. The angle of exit was 18 degrees, which is well within the requirements specified by the NCHRP Report 350. The sequential pictures showing the position of the vehicle, the deformation to the guardrail, and exit conditions of the vehicle can be seen in Figure 15. Guardrail deflection of the improved system was similar to other conventional strong-post guardrail systems. Maximum lateral deformation experienced by posts at ground level was 398 mm, which corresponds well with strong post rectangular/post W-beam guardrail post deformations [15].

Throughout the simulation, the vehicle remained upright and did not return to traffic lanes. As shown in Figure 16, damage to the vehicle was minimal. Even though the W-beam was subjected to the same dynamic loading, the W-beam rail splices at the impact region did not show any yielding or tearing. Detailed investigation at critical post locations revealed that the sacrificial rail pieces performed as intended in protecting the W-beam against bending forces. This behavior proved the importance of using sacrificial rail pieces in steel post-offset block systems. On the other hand, the necessity of moving the W-beam splices to the post mid-span can be further investigated. The accelerations measured from the vehicle were well within the acceptable acceleration limits given by NCHRP Report 350. As shown in Figure 15, results were encouraging and, based on the changes made to the system, satisfied the NCHRP Report 350 test 3-11 requirements. Clearly, further full-scale crash tests are necessary to substantiate LS-DYNA predictions.

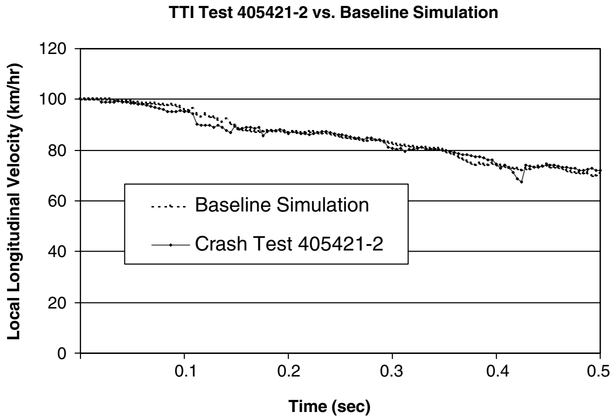

Figure 12. Comparison of local longitudinal velocity-time histories for baseline simulation: Full-scale crash test 405421-2.

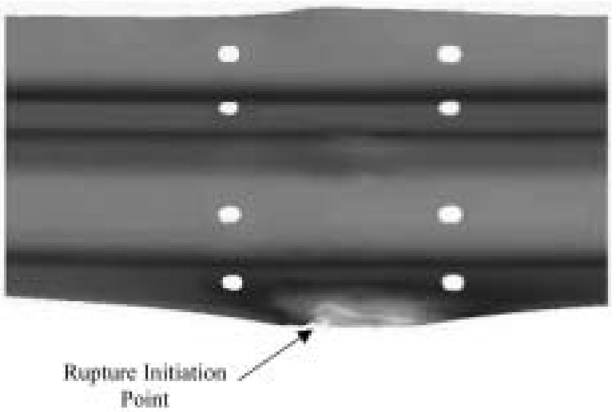

Figure 13. W-beam rupture initiation point at W-beam splice on post 19.

10. Comments

This paper shows the capabilities of finite element analysis in saving the time and resources over full-scale crash testing to an extent. Even though the finite element analysis attempts to replicate actual dynamic interactions and mechanics of an impact, there are always approximations that may introduce slight error into the model. For example, in the models under consideration, post-soil interaction, which is critical in such a study, has been represented with nonlinear elastic springs, a simplification that is widely accepted [10]. Now, however, with the advances in soil models (which are still too computationally demanding to model), the accuracy of these springs should be reevaluated to see if more approximations are needed.

Several other approximations were also used in the simulation study. These include boundary conditions, post-to-

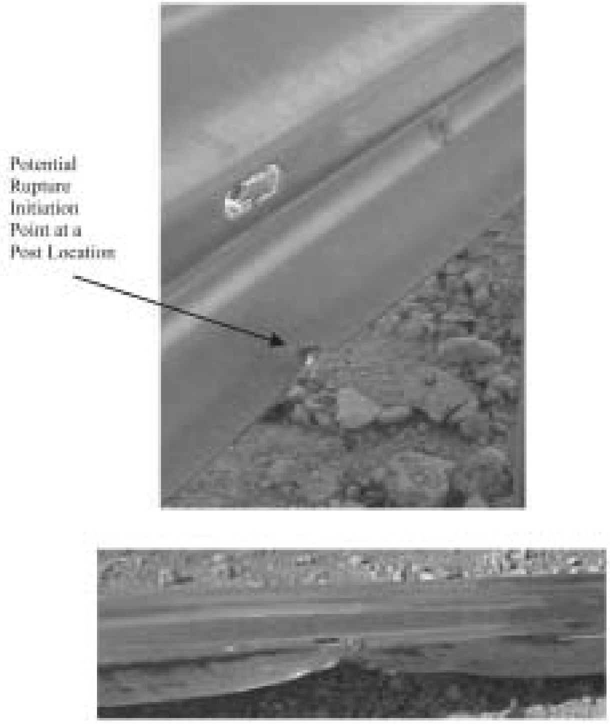

Figure 14. Picture of potential W-beam rupture initiation location.

W-beam connections, the W-beam rail splice model, and so on. Due to limitations both in time and resources, these types of approximations will always be included in a simulation study. However, the accuracy of these approximate models in representing real-world conditions should always be evaluated by means of mesh convergence studies or physical tests to limit the error introduced to simulation.

It is important to note that most real-world accidents show little resemblance to full-scale crash tests, which represent ideal conditions. Effects of roadside slopes, the positive or negative inputs of drivers during an impact, the effect of impact location, and many issues similar to these can change the outcome of an accident. With the use of advanced finite element codes and available roadside safety hardware models whose accuracy was validated against full-scale crash tests, various impact scenarios that are otherwise very difficult or impossible to conduct can be studied. A library of validated finite element models that are available to the public was provided by the National Crash Analysis Center (www.ncac.gwu.edu) to aid researchers in their simulation studies. It is believed that with the widespread use of advanced finite element codes and increased experience of the roadside safety community with the simulation technology, the concern regarding the accuracy of the finite element models and their representation of reality will dissolve in time.

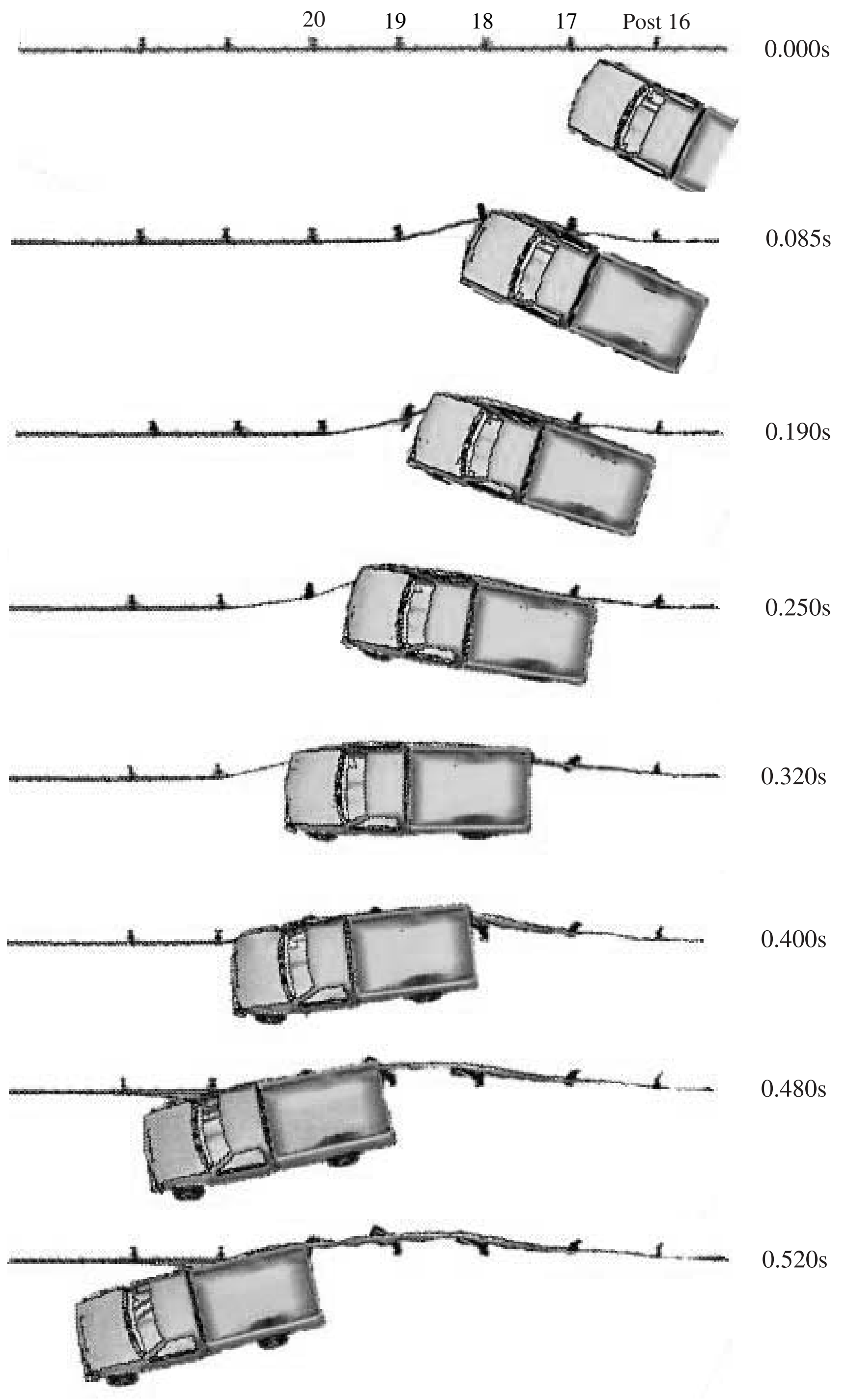

Figure 15. Sequential pictures of the second simulation study on the G4(1S) system.

Figure 16. Damage to the vehicle after the second simulation study.

11. Summary and Conclusions

In this study, an explicit three-dimensional nonlinear finite element code, LS-DYNA, was used to demonstrate how computer simulations could be used to supplement full-scale crash testing in a cost-effective manner. The results of a previously conducted full-scale crash test of a failed strong-post guardrail system were used in the study. Before the next full-scale crash test on the system, LS-DYNA was used to simulate the failed system, pinpoint the cause of the failure, and develop possible solutions to the system. After incorporating the necessary improvements, a second simulation study was performed on the system to evaluate the effect of new design changes on the performance. The results demonstrated that the system performed much better compared to the original design when the W-beam splice region was shifted from a post to mid-span location and the W-beam was protected from sharp edges of the steel post.

The capability of the computer simulation technology in evaluating and improving the impact performance of roadside safety features was also demonstrated. From the simulation technology point of view, it can be concluded that although the increasingly more sophisticated finite element codes and advanced computer hardware cannot replace experiments altogether, this technology has the potential to reduce the number of full-scale crash tests.

12. Acknowledgments

The author is indebted to Dr. Chuck Plaxico and Dr. Malcolm Ray at WPI for their help in developing finite element models and ideas for improvement and Dr. Akram Abu-Odeh at TAMU for his help with LS-DYNA simulation studies.

13. References

[1] Sicking, D. L. 1995. Applications of simulation in design and analysis of roadside safety features. Transportation Research Circular 435, TRB, National Research Council, Washington DC.
[2] Hallquist, J. O. 1998. *LS-DYNA users manual*. Livermore, CA: Livermore Software Technology Corporation.
[3] Ross, H. E., Jr., D. L. Sicking, R. A. Zimmer, and J. D. Michie. 1993. Recommended procedures for the safety performance evaluation of highway features. NCHRP Report 350, National Research Council, Washington, DC.
[4] European Standard. 1998. Road restraint systems—Part 1: Terminology and general criteria for test methods. EN 1317-1, European Committee for Standardization, Brussels, Switzerland.
[5] Atahan, A. O. 2001. Use of LS-DYNA in roadside safety. *Proceedings of the Turkish Road and Traffic Safety Congress*, Gazi University, Ankara, Turkey.
[6] Buth, E. C., R. A. Zimmer, and W. L. Menges. 1999. Testing and evaluation of a modified G4(1S) guardrail with W150 × 17.9 steel blockouts. TTI Report No. 405421-2, Texas Transportation Institute, Texas A&M University System, College Station, TX.
[7] Wright, A. E., and M. H. Ray. 1996. Characterizing guardrail steel for LS-DYNA simulations. Transportation Research Record 1528, Transportation Research Board, Washington, DC.
[8] Ray, M. H., and G. S. Patzner. 1997. Finite element model of modified eccentric loader terminal (MELT). Transportation Research Record 1599, National Academy Press, Transportation Research Board, Washington, DC.
[9] Habibagahi, K., and J. A. Langer. 1985. Horizontal subgrade modulus of granular soils. In *Laterally loaded deep foundations*, edited by J. A. Langer, E. T. Mosley, and C. D. Thompson, 21-34. Philadelphia: American Society for Testing Materials.
[10] Plaxico, C., G. S. Patzner, and M. H. Ray. 1997. Finite element modeling of guardrail timber posts and the post-soil interaction. Paper No. 980791, Transportation Research Board, Washington, DC.
[11] Ray, M. H., K. Engstrand, C. A. Plaxico, and R. G. McGinnis. 2001. Improvements to the weak-post W-beam guardrail. Paper No. 012282, Transportation Research Board, Washington, DC.
[12] Atahan, A. O. 2003. Computer simulation of recycled content guardrail posts. *Journal of Transportation Engineering*. In press.
[13] Zaouk, A. K., N. E. Bedewi, C. D. Kan, and D. Marzougui. 1996. Development and evaluation of a C-1500 pickup truck model for roadside hardware impact simulation. Paper presented at the International Mechanical Engineering Congress and Exposition, June, Atlanta, GA.
[14] Buth, E. C., W. L. Menges, and S. K. Schoeneman. 2000. NCHRP Report 350 test 3-11 on the modified PennDOT type 2 guardrail—Test 3. TTI Test No. 473750-2, Texas Transportation Institute, Texas A&M University, College Station, TX.
[15] Mak, K. K., R. P. Bligh, and W. L. Menges. 1995. Crash testing and evaluation of existing guardrail systems. Report No. 471470-26, Texas Transportation Institute, College Station, TX.

Ali O. Atahan *is an assistant professor in the Department of Civil Engineering at Mustafa Kemal University, Hatay, Turkey.*